

## Humidity Affects the Morphology of Particles Emitted from Beclomethasone Dipropionate Pressurized Metered Dose Inhalers

James W. Ivey<sup>1</sup>, Pallavi Bhambri<sup>1</sup>, Tanya K. Church<sup>3</sup>, David A. Lewis<sup>3</sup>, Mark T. McDermott<sup>2</sup>, Shereen Elbayomy<sup>2</sup>, Warren H. Finlay<sup>1</sup>, Reinhard Vehring<sup>1\*</sup>

<sup>1</sup> University of Alberta, Department of Mechanical Engineering, Edmonton, AB, Canada

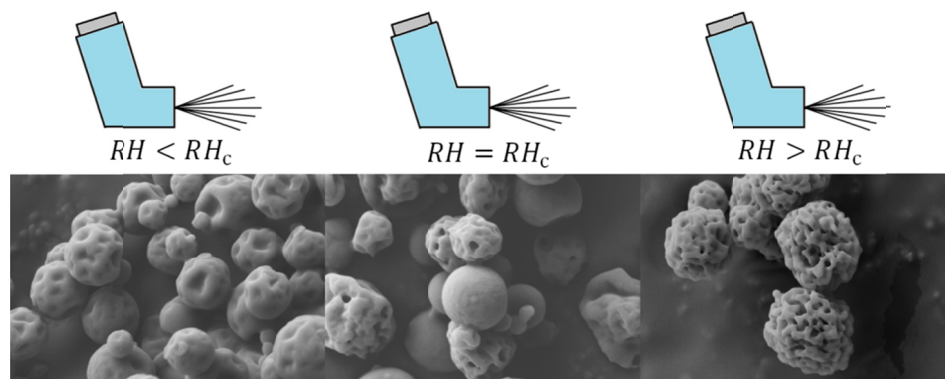
<sup>2</sup> University of Alberta, Department of Chemistry, Edmonton, AB, Canada

<sup>3</sup> Chiesi Limited, Chippenham, Wiltshire, United Kingdom

\* Corresponding author. Tel.: +1 780 492 5180; Fax: +1 780 492 2200; Email: reinhard.vehring@ualberta.ca ; Post: Reinhard Vehring, University of Alberta, Department of Mechanical Engineering, 10-269 Donadeo Innovation Centre for Engineering, Edmonton, Alberta, Canada T6G 2G8

**Keywords:** solution metered dose inhaler, pulmonary drug delivery, microparticle formation, morphology, solid phase

### Graphical Abstract



### 1. Abstract

The effects of propellant type, cosolvent content, and air humidity on the morphology and solid phase of the particles produced from solution pressurized metered dose inhalers containing the corticosteroid beclomethasone dipropionate were investigated. The active ingredient was dissolved in the HFA propellants 134a and 227ea with varying levels of the cosolvent ethanol and filled into pressurized metered dose inhalers. Inhalers were actuated into an evaporation chamber under controlled temperature and humidity conditions and sampled using a single nozzle, single stage inertial impactor. Particle morphology was assessed qualitatively using field emission scanning electron microscopy and focused ion beam-helium ion microscopy. Drug solid phase was assessed using Raman microscopy. The relative humidity of the air during

inhaler actuation was found to have a strong effect on the particle morphology, with solid spheroidal particles produced in dry air and highly porous particles produced at higher humidity levels. Air humidification was found to have no effect on the solid phase of the drug particles, which was predominantly amorphous for all tested formulations. A critical level of air relative humidity was required to generate porous particles for each tested formulation. This critical relative humidity was found to depend on the amount of ethanol used in the inhaler, but not on the type of propellant utilized. The results indicate that under the right circumstances water vapor saturation followed by nucleated water condensation or ice deposition occurs during particle formation from evaporating propellant-cosolvent-BDP droplets. This finding reveals the importance of condensed water or ice as a templating agent for porosity when particle formation occurs at saturated conditions, with possible implications on the pharmacokinetics of solution pMDIs and potential applications in particle engineering for drug delivery.

## 2. Introduction

Inhaled corticosteroids are widely prescribed for prophylactic asthma therapy (Busse, 2002) and may also benefit patients with moderate to severe chronic obstructive pulmonary disease (Gartlehner et al., 2006). A large proportion of inhaled corticosteroid doses are delivered using pressurized metered dose inhalers (pMDIs) (Lechuga-Ballesteros et al., 2011; Roche and Dekhuijzen, 2016). In modern pMDIs, the drug is either suspended or dissolved in a volatile hydrofluoroalkane (HFA) propellant, with the choice dependent on the solubility of the drug in the propellant (Myrdal et al., 2014); the inhaled corticosteroid beclomethasone dipropionate (BDP) has generally been formulated as a solution (Spahn, 2016) utilizing ethanol as a co-solvent (Gupta et al., 2003). The resulting formulation is contained in a pressurized canister equipped with a metering valve and paired with an actuator (Stein et al., 2014). When a patient administers a dose from a pMDI, the volatile formulation exits the valve via the actuator and is atomized into a fine, rapidly evaporating spray which is inhaled into the patient's lungs (Finlay, 2011).

The aerodynamic particle size distribution of a therapeutic aerosol has a large effect on the efficacy of treatment in pulmonary delivery because of its prominent role in the physical mechanisms of particle deposition in the human airways (Darquenne, 2012). Consequently, a substantial amount of research on pMDIs has focused on measurement and prediction of the drug particle size distribution for solution and suspension formulations. The matter is complicated by the highly dynamic nature of the aerosol generated by pMDIs: as the spray of propellant droplets interacts with the surrounding gas phase, heat, mass, and momentum are transferred (Xu and Hickey, 2014), and thus the velocity, size, and concentration of droplets vary in time and space (Dunbar et al., 1997). Available theory (Finlay, 2001) suggests that the formulation (propellant physical properties, inclusion of co-solvent) and usage environment (air temperature, relative humidity) have the potential to alter these spray dynamics and therefore the deposition in human

airways. Indeed, *in vitro* studies summarized in our recent review (Ivey et al., 2015) have demonstrated all of these effects.

As the interaction of pMDI-generated aerosols with humidity is of particular relevance to the present study, a brief survey of research on this topic is merited. Evaporative cooling in pMDI spray plumes can produce temperatures well below 0 °C (Brambilla et al., 2011), and the plume may contain as many as hundreds of millions of microparticles (Stein, 2008). If the air entrained into the pMDI spray plume is sufficiently humid, these conditions might produce supersaturation of water vapor and subsequent nucleated condensation of water (Hinds, 1999). An early evaluation of the effect of humidity on the aerodynamic particle size distribution of nine commercial chlorofluorocarbon pMDIs was conducted by Kim et al. (Kim et al., 1985). Testing was conducted with air conditioned to 22-23 °C and either < 1% or 90% relative humidity (RH). A 20 liter evaporation chamber was employed upstream of an Andersen cascade impactor to measure the aerodynamic particle size distribution of the fully evaporated aerosols. No significant effect of RH on the aerodynamic particle size distribution for eight of the nine tested inhaler types was observed when the RH was increased from near zero to 90%, and thus it was concluded that for the tested pMDIs humidity did not alter the particle size distribution of the aerosol reaching the impactor. In a later study, Lange and Finlay administered doses from an HFA-propelled suspension pMDI to a model ventilation circuit equipped with a pediatric endotracheal tube coupled to an Andersen cascade impactor (Lange and Finlay, 2000). Ventilation air was supplied at 4.8 L/min with a square wave profile. Ventilation air temperature was varied from 25 °C to 37 °C, and was either unhumidified (RH 8-15%) or humidified to near saturation (RH ≈ 100%). The *in vitro* inhaled dose was observed to depend heavily on the amount of water vapor present in the ventilation air (i.e. the absolute humidity), with the inhaled dose decreasing as the water vapor mole fraction increased. Importantly, Lange and Finlay observed that the aerodynamic particle size distribution of the aerosol passing the endotracheal tube was unaffected by changes in air humidity and that the deleterious effect of humidity on the *in vitro* inhaled dose was mitigated when a spacing device was added to the ventilation circuit prior to the endotracheal tube and impactor. This data suggests that humidity could affect particle sizes in the spacer immediately after droplet production. In a subsequent study designed to further examine the effect of humidity, Martin et al. examined the evaporation rate of millimeter size pendant propellant-ethanol droplets in air with varying humidity levels (Martin et al., 2005). They found no effect of air humidity on droplet evaporation rates.

Evidence that humidity can alter the aerodynamic particle size distribution from pMDIs was published by Mitchell and colleagues, who utilized an Andersen cascade impactor with an endotracheal tube fixed to the inlet to evaluate the effect of air humidity on the aerodynamic particle size distribution of BDP solution pMDIs paired with valved holding chambers (Mitchell et al., 2003). They found that increasing the absolute humidity of the testing air resulted in a large increase in the mass median aerodynamic diameter (MMAD) for an HFA BDP pMDI and

concluded that the effect was due to growth by condensation of the aerosol particles generated by the inhaler. Martin and Finlay sized salbutamol sulfate suspension pMDIs actuated into valved holding chambers in 37 °C air using an Andersen cascade impactor; to evaluate any effects related to aerosol maturation, they varied the distance between the holding chamber and the impactor by using different lengths of connecting tubing (Martin and Finlay, 2005). They found that increasing the RH from 8% to near 100% resulted in significant increases in holding chamber deposition and MMAD for a conventional formulation containing ethanol and surfactant as well as for an excipient-free formulation. Furthermore, in humidified air the MMAD was observed to decrease significantly as the spacing tubing length was increased. Martin and Finlay's results suggest that significant condensational growth of pMDI drug particles occurs at high air relative humidity, and that this growth is followed by secondary evaporation of the condensed water. This idea is consistent with the prior results: if the aerosol is given sufficient time to mature (as with the large volume evaporation chamber of Kim et al. or the low sampling flow rate employed by Lange and Finlay), any transient size increases will be undetectable by typical particle sizing techniques, as secondary evaporation will have taken place prior to sizing. On the other hand, if the sizing occurs while condensational size changes are still underway (as with the studies of Mitchell et al. and Martin and Finlay), the measured aerodynamic particle size distribution will depend on how far along the aerosol maturation process has progressed. Thus, although condensational growth and secondary evaporation of pMDI-generated aerosols have not been observed directly, the available research provides indirect evidence that these phenomena do indeed occur.

Recently, researchers studying solution pMDIs have focused attention on particle properties other than the aerodynamic particle size distribution. Notably, the solid phase and the particle morphology become important after particle deposition in the airways (de Souza Carvalho et al., 2014), as they may affect particle wettability, dissolution rate, and susceptibility to the lungs' particle clearance mechanisms (Ruge et al., 2013). The solid phase of inhaled drugs has been shown to affect pharmacokinetics and pharmacodynamics in animal models (Sakagami et al., 2002; Sakagami et al., 2001). This is a relevant consideration since unlike in suspension formulations, the drug in a solution pMDI undergoes a rapid transition from a solute to a solid during dosing, with the resultant solid phase potentially dependent on the formulation and usage environment. Therefore, some recent research has evaluated the effects of formulation variables (ethanol content, presence of excipients) on the solid phase and the resultant dissolution and transport characteristics of the drug particles. Grainger and colleagues evaluated two commercially available BDP pMDIs, distinguished by ethanol content and use of the excipient glycerol (Grainger et al., 2012). They found that the glycerol-containing formulation differed significantly from the glycerol-free formulation in its extent of crystallinity, dissolution rate, and *in vitro* transcellular absorption. Similar findings were reported in work by Lewis, Haghi, and colleagues (Haghi et al., 2014; Lewis et al., 2014). Further studies with BDP solution pMDIs

(Buttini et al., 2014) and with model propellant systems (Bouhroum et al., 2010; Ooi et al., 2014) indicate that BDP may form solvates or clathrates with ethanol or propellants during drug particle formation.

The morphology of a drug particle may alter its fate after deposition in the lungs as well. Specifically, particle density (Tsapis et al., 2002) and wettability (Schürch et al., 1990) have the potential to affect the rate of particle dissolution or clearance in the airways. Zhu et al. investigated the effect of ethanol content on the morphology of particles generated from budesonide solution pMDIs (Zhu et al., 2013). Utilizing field emission scanning electron microscopy (FE-SEM) and focused ion beam milling-scanning electron microscopy (FIB-SEM), they found that ethanol content had a large effect on the particle morphology. Particles produced from pMDIs with a low ethanol content tended to have an irregular envelope shape and a porous morphology, while those produced from pMDIs with more ethanol were generally smooth, solid, and spheroidal. In a subsequent study, similar morphological transitions related to ethanol content were observed for both BDP and fluticasone propionate solution pMDIs (Zhu et al., 2014). Porous BDP particles have also been observed by other researchers (Buttini et al., 2014; Grainger et al., 2012; Lewis et al., 2014). In the present study, we build on these findings by investigating the effect of propellant type and air humidity on the morphology and solid phase of the particles produced by BDP solution pMDIs.

### **3. Materials and Methods**

#### **3.1. pMDI Filling and Particle Sampling**

BDP solution pMDIs were prepared by first weighing out and dissolving beclomethasone dipropionate (Chiesi Farmaceutici, Parma, Italy) in anhydrous reagent grade ethanol. The resulting concentrated solutions were added to 19 mL aluminum aerosol canisters with a fluoropolymer internal coating (Presspart Ltd, Blackburn, UK). Canisters were capped with 50  $\mu$ L metering valves (BK357, Bepak Ltd, Kings Lynn, UK) and then crimped and filled with a metered volume of propellant using a lab-scale aerosol container crimper-filler (Lab Plant, Pamasol AG, Pfäffikon, Switzerland). Each inhaler was filled to a target solution volume of 10 mL with a target BDP concentration of 2 mg/mL and paired with a polymer actuator with a nominal actuator orifice diameter of 0.30 mm (Presspart Ltd, Blackburn, UK). Both HFA propellants p134a (Linde, Mississauga, Canada) and p227ea (Mexichem Fluor, Runcorn, UK) were assessed. Formulations are summarized in Table 1.

Table 1: Summary of the formulation variables for the four tested BDP solution formulations.

Formulation Identifier	Propellant type	Ethanol Content (% w/w)	BDP Metered Dose ( $\mu\text{g}$ )
134_5	134a	5	100
134_18	134a	18	90
227_5	227ea	5	100
227_18	227ea	18	100

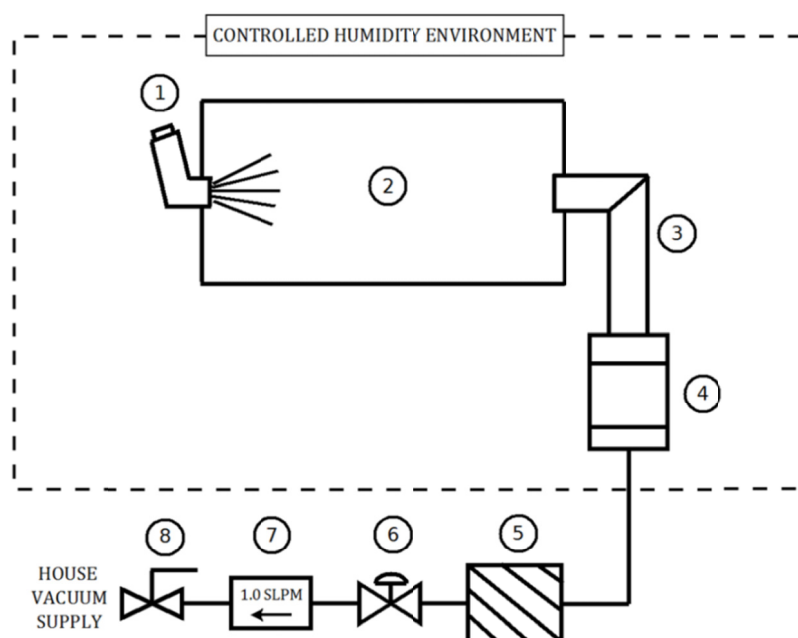


Figure 1: Schematic of the controlled humidity particle sampling setup used in this work. (1) BDP solution pMDI (2) 9 liter polypropylene evaporation chamber (3) USP induction port (4) Single stage, single nozzle impactor, cut size  $0.6 \mu\text{m}$  at 1.0 SLPM air flow rate (5) Inline HEPA filter (6) Flow control valve (7) Flow meter (8) Shutoff valve

The experimental setup for pMDI particle sampling at controlled humidity conditions is shown schematically in Figure 1. Humidity control was achieved by situating the test apparatus inside an enclosed environment and conducting testing therein. For humidified conditions ( $\text{RH} \geq 8\%$ ), an environmental chamber (Lunaire, White Deer, PA, USA) maintained the temperature at  $20.0 \pm 0.5 \text{ }^\circ\text{C}$ , and the RH to within  $\pm 1 \%$  of set point (95% confidence interval). For tests at very dry conditions, a glove box with dry gas purge (Terra Universal, Fullerton, CA, USA) was better able to maintain the dry environment; dry tests were conducted at  $22.0 \pm 1.0 \text{ }^\circ\text{C}$ , with  $\text{RH} \leq 2\%$  in all cases. A translucent polypropylene box with a volume of 9 liters served as an evaporation chamber; it was modified to allow a pMDI mouthpiece adapter to be ported at one

end. A USP induction port (USP, 2013) was fitted at the other end. The downstream end of the USP induction port was coupled to a custom, single nozzle, single stage impactor (Wang, 2015) configured with a nozzle diameter of 0.6 mm, a nozzle-to-collection-plate distance of 2.5 mm, and a calculated cut size of 0.6  $\mu\text{m}$  at a nominal flow rate of 1.0 SLPM. The impactor utilized standard 12.7 mm diameter ultramicroscopy pin mounts (Ted Pella, Redding, CA, USA) as removable collection plates. Samples for ultramicroscopy were collected onto double-sided adhesive conductive carbon tabs (Ted Pella, Redding, CA, USA) affixed to pin mounts; samples for spectroscopy were collected onto bare aluminum pin mounts that had been cleaned by double washes in reagent grade acetone and methanol. The sampling flow rate was set by means of a needle valve and monitored with a gas mass flow meter (Model 4043, TSI, Shoreview, MN, USA); it was maintained at  $1.00 \pm 0.05$  SLPM for all tests. For each sample collection, a single priming shot was fired into a waste flask and then 5-10 shots from the pMDI were administered into the evaporation chamber, with a pause of approximately one second between each shot. Then a  $10 \pm 1$  second holding period to allow aerosol maturation was followed by 5 minutes of aerosol sampling. Given the multitude of actuations, the length of the sampling period, and the cut size of the impactor, the sampled fraction was expected to be adequately representative of the entire aerosol. After the sampling period, the impactor was disassembled and particle-laden pin mounts were transferred to a specimen box with a desiccant sachet to await analysis. The USP induction port and the impactor components were cleaned with ethanol and lint-free wipes between every measurement.

### **3.2. BDP Particle Morphology by FE-SEM, FIB-HIM**

Samples were coated in gold by sputter deposition (Desk II, Denton Vacuum, Moorestown, NJ, USA) for 120 seconds at 15-20 mA current, resulting in a coating thickness of approximately 20 nm. Samples were imaged using FE-SEM (Sigma FE-SEM, Zeiss, Jena, Germany) with an accelerating voltage of 3-5 kV and a 30  $\mu\text{m}$  lens aperture. Secondary electrons were detected with the out-of-lens detector. Selected samples were also analyzed using focused gallium ion beam milling and helium ion microscopy (Ga-FIB-HIM) (Orion NanoFab, Zeiss, Jena, Germany). Particles were sectioned with a gallium ion beam (30 kV accelerating voltage, 50 pA beam current, 40  $\mu\text{m}$  aperture) and then imaged by helium beam (30 kV accelerating voltage, 1 pA beam current). Analysis of Ga-FIB-HIM micrographs was conducted with image analysis software (ImageJ, NIH, Bethesda, MD, USA).

### **3.3. BDP Solid Phase by Raman Microscopy**

Due to the small sample mass contained in each dose, Raman microscopy was selected to assess the solid phase of BDP pMDI samples. This allowed preparation of samples with adequate Raman signal while consuming only 5-10 shots from each inhaler. Samples were analyzed by placing particle-laden pin mounts directly onto the stage of a Raman microscope (inVia, Renishaw, Prospect Scientific, Ontario, Canada). An argon ion laser with a 514.5 nm

wavelength was operated at 5 mW and focused through a 20x objective lens to a spot size of roughly 5  $\mu\text{m}$ . The Raman spectrum from 2100-3600  $\text{cm}^{-1}$  was acquired with a spectral resolution of approximately 1.5  $\text{cm}^{-1}$ . A moderate fluorescence background was present in many spectra; this was subtracted using software (Origin 2015, OriginLab, Northampton, MA, USA). Since the low-frequency shift region of the spectrum was inaccessible due to the configuration of the instrument optics, the degree of crystallinity was assessed qualitatively by comparison to the spectra of crystalline and amorphous standards in the C-H stretch band around 3000  $\text{cm}^{-1}$  (top two spectra in Figure 4). The spectrum of the anhydrous microcrystalline BDP raw material was used as the crystalline standard. An amorphous BDP standard was generated by spray drying monodisperse droplets of BDP dissolved in HFA 134a-ethanol at a very low liquid flow rate at near room temperature to produce a dried powder sample; the powder production method is described in detail elsewhere (Azhdarzadeh et al., 2016). Low frequency shift Raman spectroscopy was utilized as a complementary technique to verify the solid phase of the standard materials; this technique has been shown to be extremely sensitive to the level of intramolecular order and thus degree of crystallinity (Hédoux et al., 2011). A spectral comparison of the dried powder and crystalline samples was conducted using techniques and equipment similar to those described in previous work (Wang et al., 2014). Briefly, analysis of the BDP standards was conducted on a custom macro Raman system. A comparison of the low frequency shift band of the spectra is presented in Figure 2. The dried powder sample displayed an absence of the peaks corresponding to crystalline lattice vibrations present in the crystalline standard. This comparison suggested that the dried powder sample was highly amorphous, and it was thus selected as the spectral standard for amorphous BDP.

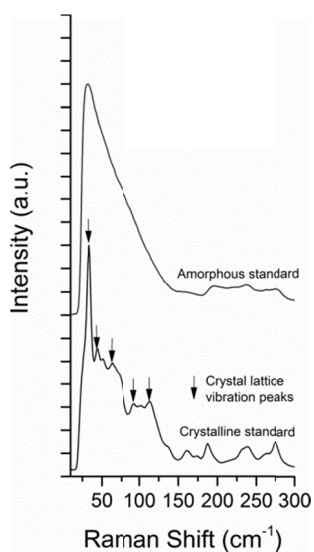


Figure 2: Raman spectra of amorphous and crystalline BDP standards in the low frequency shift region. Spectra are offset vertically.



#### 4. Results and Discussion

The aim of the first round of inhaler testing was to qualitatively assess the impact of formulation and air humidity on the morphology and solid phase of the BDP particles. Selected FE-SEM micrographs of all four pMDI formulations actuated in very dry ( $RH \leq 2\%$ ) or humid ( $RH = 38 \pm 1\%$  for p227ea inhalers or  $RH = 50 \pm 1\%$  for p134a inhalers) air are presented in Figure 3. BDP particles generated from pMDIs actuated in dry air (leftmost four panels in Figure 3) were generally spheroidal, with numerous submicron surface concavities. Some particles displayed a single larger concavity as well. Overall, little effect of propellant type or ethanol content on the particle morphology was observed.

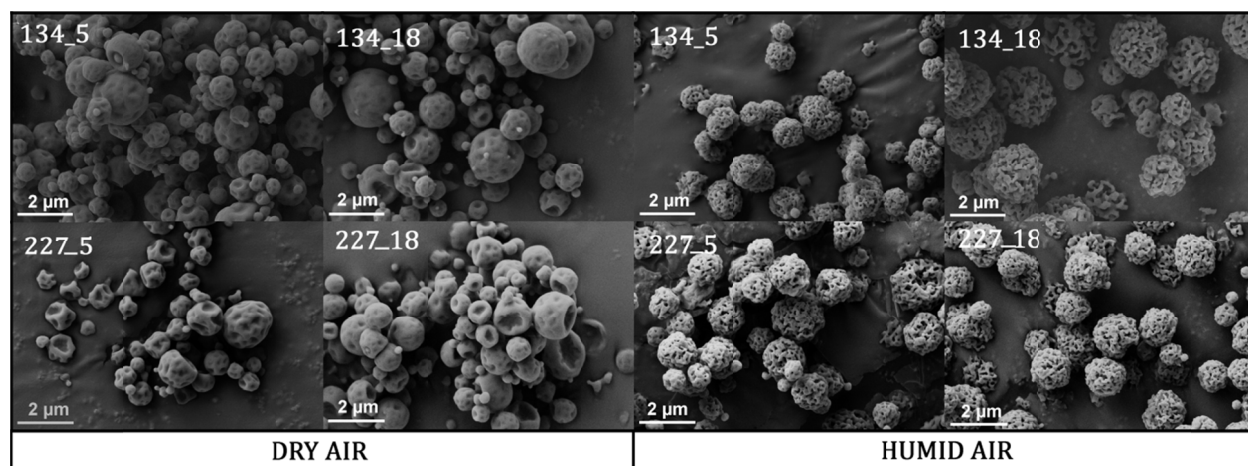


Figure 3: Selected FE-SEM micrographs of all four BDP formulations actuated in dry air (leftmost four panels) or humid ( $RH = 38 \pm 1\%$  for p227ea inhalers or  $RH = 50 \pm 1\%$  for p134a inhalers) air (rightmost four panels).

For all tested pMDI formulations, the presence of humidity in the air substantially altered the morphology of the BDP particles. While the size and envelope shape of the particles appeared similar regardless of humidity, extensive pores with characteristic dimension on the order of 100 nm were present in the particles produced in humid air. Figure 4 offers a closer view of particles produced by pMDI 134\_5 in dry (left) or humid (right) conditions. Micrographs of single particles produced by pMDI 227\_5 after cross-sectioning using FIB-HIM are shown in Figure 5. Unlike the almost entirely solid particle produced in dry air, the BDP particle produced in humid air (right panel) contains pores throughout the entire cross section. These results indicate that a minimal level of water vapor in the air is required to produce pores in the BDP microparticles, and that the pore former must be condensed water or ice. Further, the abundance of pores throughout the particle cross-section observed in Figure 5 suggests that pore formation occurs while particle drying and surface recession are still underway; otherwise we would expect pores to be confined to the near-surface region of the particles. The pores make up an appreciable fraction of the particle volume. The area occupied by pore space and the total cross section of the porous particle in the right hand panel of Figure 5 were estimated using image

analysis software. Taking the ratio of these two quantities yielded a rough estimate for the particle void fraction of 0.2. This allows estimation of the effect of humidity-induced pore formation on the MMAD of the aerosol. For a solution pMDI, the MMAD of the residual aerosol after the liquid phase is fully evaporated is related to the mass median diameter of the spray of droplets from which it formed,  $MMD_d$ , by

$$MMAD \cong \sqrt[3]{\frac{c}{\rho^*}} \sqrt[6]{\frac{\rho_p}{\rho^*}} MMD_d$$

where  $c$  is the concentration of solids in the droplet,  $\rho_p$  is the particle density, and  $\rho^*$  is a reference density of  $1000 \text{ kg/m}^3$  (Ivey et al., 2014). For a porous particle, the particle density is related to the void fraction  $\phi$  by

$$\rho_p = (1 - \phi)\rho_t$$

where  $\rho_t$  is the bulk or true density of the matrix material (Dullien, 1992). Taking the ratio of the MMAD of an aerosol comprising porous particles where the condensed pore former has fully evaporated to that of an aerosol produced by the same spray and consisting of solid particles with  $\rho_p = \rho_t$  then gives

$$\frac{MMAD_{\text{porous}}}{MMAD_{\text{solid}}} \cong \sqrt[6]{1 - \phi}$$

This result indicates that very extensive porosity is required to substantially alter the MMAD of solution pMDI aerosols due to the weak sixth-root dependence on void fraction. The level of porosity seen in the right panel of Figure 5, and generally in particles produced under humid conditions in this study, is unlikely to meaningfully alter the MMAD of the aerosol relative to the nonporous particles produced under dry conditions. As discussed in the introduction, pMDI aerosols may undergo condensational growth and secondary evaporation depending on environmental conditions, and these processes may still be underway as particles deposit in sizing equipment or human airways. Thus the effects of environmental conditions on *in vitro* deposition observed by other researchers are more likely attributable to the extent to which aerosol maturation has progressed than to humidity-related alterations to particle morphology.

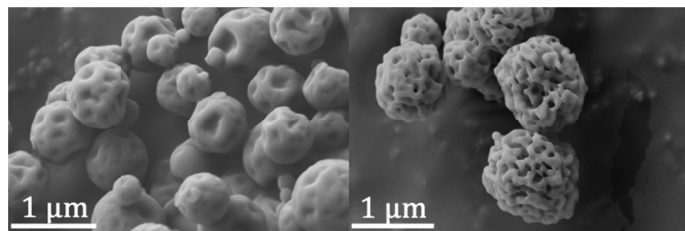


Figure 4: FE-SEM micrographs of BDP particles produced from the 5% w/w ethanol, p134a pMDI. Left panel: air RH  $\leq$  2%. Right panel: RH =  $50 \pm 1\%$ .

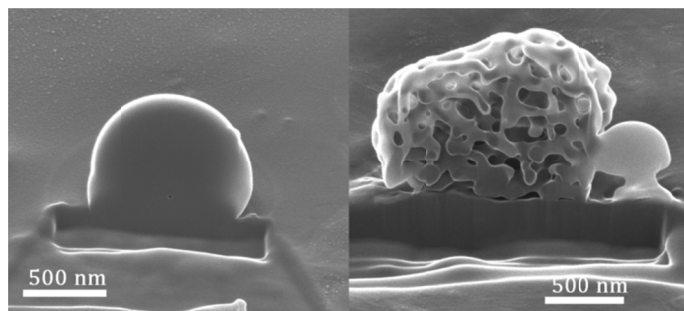


Figure 5: FIB-HIM micrographs of particles produced by the 5% ethanol, p227ea pMDI. Left panel: air RH  $\leq$  2%. Right panel: air RH =  $38 \pm 1\%$ .

The micro-Raman spectra of all four formulations tested in dry and humidified air are presented in Figure 6, along with the spectra of the crystalline and amorphous standards. The spectra of the pMDI-produced powders are very similar to the amorphous standard regardless of formulation or level of humidity in the air, indicating that BDP pMDIs produce predominantly amorphous particles; this is consistent with the results of other researchers (Lewis et al., 2014; Zhu et al., 2014). In a sample that had been stored in a desiccator for three weeks prior to analysis (bottom spectrum in Figure 6), a characteristic peak at  $2996\text{ cm}^{-1}$ , which is prevalent in the crystalline standard, appeared, suggesting that some crystallization had occurred during storage. This finding is somewhat surprising: since the unplasticized glass transition temperature of amorphous BDP has been reported as approximately  $65\text{ }^{\circ}\text{C}$  (Abdel-Halim et al., 2011), available theory suggests the amorphous phase should be fairly stable at room temperature (Hancock et al., 1995). Other research demonstrates that ethanol may alter the solid phase of BDP produced by solution pMDIs (Buttini et al., 2014). It is possible that the solid phase change observed during storage is related to residual ethanol content or the presence of a crystalline fraction in the form of nanocrystalline nuclei. Regardless of the source of the instability, given the similarity of the solid phase of the porous and the non-porous particle samples, it appears unlikely that crystallization of BDP is responsible for pore formation.

Additional experiments were conducted to identify the critical air relative humidity required for pore formation,  $RH_c$ . In these experiments, for a given pMDI formulation the RH of the air in the environmental chamber was increased in discrete steps and the resulting particle morphologies were assessed via SEM until a mixed population of porous and pore-free particles was observed in a single sample. An example of this approach is provided in Figure 7, where pMDI 134\_5 first yielded both porous and non-porous particles when tested at an air RH of  $14 \pm 1\%$  RH. Hence for that formulation, we concluded that  $RH_c = 14 \pm 1\%$ . The values of  $RH_c$  thus determined for each formulation are summarized in Table 2, along with the corresponding dew point temperatures. These results show that the critical RH for pore formation depends on the ethanol content in the pMDI. Any effect of propellant type is within the error of the RH measurement. For three of the four tested formulations, a more subtle morphological transition

was observed when air humidity increased from the dry ( $\leq 2\%$  RH) condition to a level slightly below  $RH_c$ . For example in Figure 8, the numerous submicron surface concavities present in particles from pMDI 134\_18 sampled from very dry air were no longer present when the same pMDI was actuated in air humidified to  $14 \pm 1\%$  RH. The rightmost column of Table 2 indicates for which formulations this phenomenon was observed. This finding suggests that in addition to forming pores, condensed water (liquid or solid) may alter the surface roughness of BDP particles.

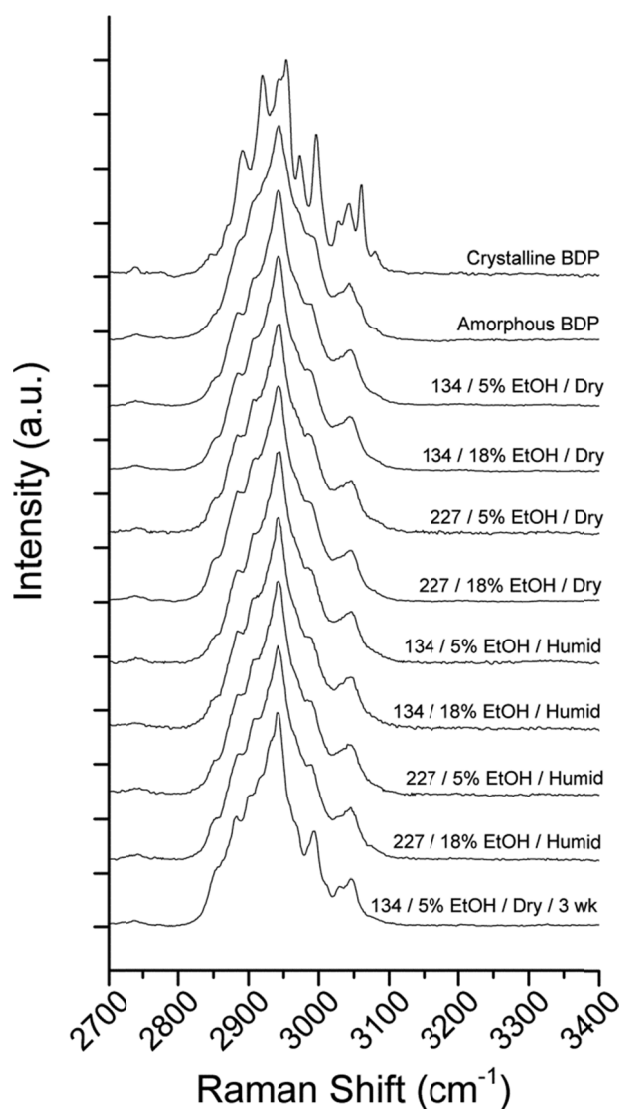


Figure 6: Raman spectra of BDP samples in the C-H stretch band. Spectra are offset vertically. Topmost two spectra: crystalline and amorphous standards. Third through tenth spectra from top: spectra from pMDI samples tested at either dry ( $RH \leq 2\%$ ) or humid ( $RH 38 \pm 1\%$  for p227ea inhalers or  $RH 50 \pm 1\%$  for p134a inhalers) air. Bottom spectrum: sample obtained from pMDI 134\_5 actuated in dry air and stored for three weeks in a desiccator at room temperature.

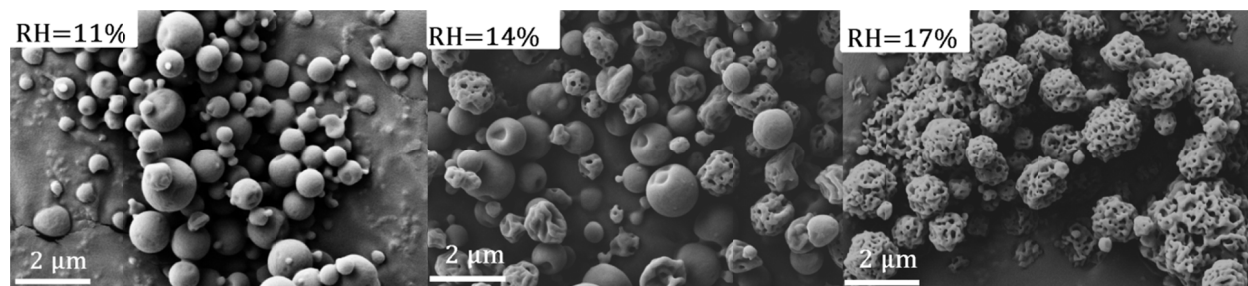


Figure 7: FE-SEM micrographs of the particles produced by pMDI 134\_5 at varying air relative humidity. In this case a mixed population of porous and non-porous particles was observed at  $14 \pm 1\%$  RH, indicating that the critical RH for pore formation  $RH_c$  lies in this range.

Table 2: Summary of the critical RH for pore formation and the corresponding dew point temperature for each of the tested BDP formulations. The rightmost column indicates whether any particle surface modification was observed below  $RH_c$ .

Formulation Identifier	Propellant type	Ethanol Content (% w/w)	$RH_c$ ( $\pm 1\%$ at 95% confidence interval)	Dew point temperature corresponding to $RH_c$ ( $^{\circ}\text{C}$ )	Particle surface smoothing for $2\% < RH < RH_c$ ?
134_5	134a	5	14	$-7 \pm 1$	Yes
134_18	134a	18	16	$-6 \pm 1$	Yes
227_5	227ea	5	14	$-7 \pm 1$	No
227_18	227ea	18	17	$-5 \pm 1$	Yes

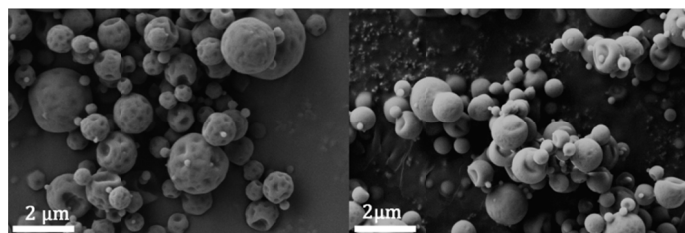


Figure 8: FE-SEM micrographs of particles sampled from pMDI 134\_18 actuated in dry (left) or  $14 \pm 1\%$  RH air.

It is interesting to place the current findings in the context of previous research by Zhu and colleagues, who separated a fraction of pMDI-produced aerosols for analysis using cascade impaction (Zhu et al., 2014). They reported a transition from porous to nonporous particle morphology with solution formulations of BDP and fluticasone propionate as pMDI ethanol content was increased. The employed particle sampling technique allowed less time for aerosol maturation prior to deposition than in this work, which may account for qualitative differences in particle morphology compared to the present study. The proposed pore formation mechanism of Zhu et al. did not include any interaction with condensed water from the surrounding air,

whereas the present study conclusively demonstrates that absent sufficient air humidity, no pores are formed in particles from BDP solution pMDIs regardless of formulation variables. In this study, we demonstrate that sufficiently humid air is a necessary condition for pore formation. The effect of ethanol content reported by Zhu et al. is likely due to ethanol's effect on  $RH_c$  as demonstrated in this work. Increasing ethanol content has been shown to slow propellant evaporation (Stein and Myrdal, 2006), which will tend to reduce evaporative cooling and generally increase the temperature of the pMDI spray plume. Therefore the degree of water vapor saturation achieved as parcels of entrained air are cooled will decrease as spray plume temperature increases. Thus the temperature and humidity of the air entrained into the pMDI spray plume and the temperature field within the spray plume itself largely determine whether water vapor saturation and subsequent morphology modification might occur.

These effects are illustrated conceptually in Figure 9. The dew point temperature—that is, the temperature at which the water vapor in air reaches saturation when cooled at constant pressure (Van Wylen and Sonntag, 1965)—of air at 20 °C and 101.3 kPa absolute pressure is plotted against the air relative humidity using a simple model (Buck, 1981). As an illustrative example, the value of  $RH_c$  determined for pMDI 134\_18 ( $16 \pm 1$  %) defines the center of a transition RH range wherein particle formation may occur either above or below the dew point temperature and thus below or above water vapor saturation. A transition range is expected rather than an abrupt transition because the temperature of pMDI spray plumes vary in time and space (Oliveira et al., 2013); this likely explains the observation of a mixed population of particle morphologies at  $RH_c$ . The intersection of this RH range with the dew point curve corresponds to a range of spray plume temperatures. Since pMDI spray plume temperatures are affected by formulation and device variables (Brambilla et al., 2011), the position and breadth of the transition RH region and the spray plume transition temperature region may respond to changes in formulation or device. Increasing ethanol content is expected to increase the spray plume temperature, which can be visualized on Figure 9 as an upward shift in the transition temperature range. This is expected to shift the transition RH region to the right and increase  $RH_c$ , as was observed in this study.

The dew point temperatures corresponding to the observed values of  $RH_c$  in Table 2 are all less than 0 °C. At these temperatures, the degree of saturation with respect to the ice phase is greater than with respect to the water phase (Hobbs, 1974). It is therefore impossible to say whether the pore formers are liquid water droplets or ice crystals without additional experimental work. Either scenario is possible given the low aqueous solubility of BDP (Sakagami et al., 2002) and the complexities of nucleated water condensation or ice deposition from the vapor phase (Hoose and Möhler, 2012). Regardless of the exact mechanism of pore formation, porosity in inhaled BDP microparticles alters both the particle density (Edwards et al., 1997) and the wettability via contact angle modification (Israelachvili, 2011). Therefore the fate of a porous

drug particle might differ from that of a smooth, solid particle after deposition in the airways, with potential implications on pharmacokinetics.

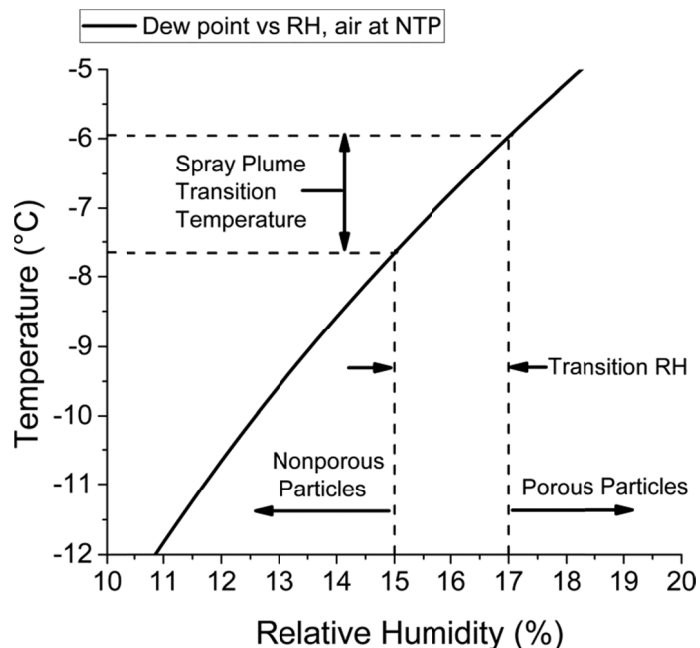


Figure 9: A plot of dew point temperature vs RH for air at normal temperature and pressure (NTP, 20 °C and 101.3 kPa), with annotations demonstrating the hypothesized effects of spray plume temperature and air RH on the resulting morphology of the particles produced by BDP solution pMDIs.

## 5. Conclusions

In this work, we demonstrate that air humidity can strongly affect the morphology of microparticles produced by solution pMDIs. Our results indicate that under the right environmental conditions, water in a condensed phase is capable of acting as a templating agent during particle formation from propellant solution droplets. This occurs at room temperature at levels of humidity that are very likely to be encountered during typical patient usage or in the clinic, and results in highly porous particles for the inhaled corticosteroid beclomethasone dipropionate. The resulting modifications to surface and internal morphology may affect particle density and wettability, with the potential to alter the way these porous drug particles interact with the human airways. While no humidity induced changes to the solid phase of BDP particles were observed in this work, this may not hold true for a more hydrophilic drug. Therefore, solution pMDI researchers and clinicians should strongly consider controlling or measuring the air humidity during experiments or trials.

These results may be of interest to researchers in the field of particle engineering for pulmonary drug delivery as well: highly porous particles have been shown to have advantageous

aerodynamic properties (Tsapis et al., 2002), low cohesive forces (Tarara et al., 2000), and excellent colloidal stability in suspension (Tarara et al., 2004) . However, producing such particles typically requires complicated formulation or processing techniques. Here, we produced porous microparticles with a relatively straightforward formulation and spray evaporation process, albeit at a very small scale.

## 6. References

- U.S. Pharmacopeial Convention, 2013. Chapter <601>: Aerosols, nasal sprays, metered-dose inhalers, and dry powder inhalers, USP 36 - NF 31. United Book Press, Baltimore, MD.
- Abdel-Halim, H., Traini, D., Hibbs, D., Gaisford, S., Young, P., 2011. Modelling of molecular phase transitions in pharmaceutical inhalation compounds: An *in silico* approach. *Eur. J. Pharm. Biopharm.* 78, 83-89.
- Azhdarzadeh, M., Shemirani, F.M., Ruzycki, C.A., Baldelli, A., Ivey, J.W., Barona, D., Church, T., Lewis, D., Olfert, J.S., 2016. An atomizer to generate monodisperse droplets from high vapor pressure liquids. *Atomization Spray* 26, 121-134.
- Bouhroum, A., Burley, J.C., Champness, N.R., Toon, R.C., Jinks, P.A., Williams, P.M., Roberts, C.J., 2010. An assessment of beclomethasone dipropionate clathrate formation in a model suspension metered dose inhaler. *Int. J. Pharm.* 391, 98-106.
- Brambilla, G., Church, T., Lewis, D., Meakin, B., 2011. Plume temperature emitted from metered dose inhalers. *Int. J. Pharm.* 405, 9-15.
- Buck, A.L., 1981. New equations for computing vapor pressure and enhancement factor. *J. Appl. Meteorol.* 20, 1527-1532.
- Busse, W., 2002. How inhaled corticosteroids changed asthma therapy, in: Schleimer, R.P., O'Byrne, P.M., Szeffler, S.J., Brattsand, R. (Eds.), *Inhaled steroids in asthma*. Marcel Dekker, New York.
- Buttini, F., Miozzi, M., Balducci, A.G., Royall, P.G., Brambilla, G., Colombo, P., Bettini, R., Forbes, B., 2014. Differences in physical chemistry and dissolution rate of solid particle aerosols from solution pressurised inhalers. *Int. J. Pharm.* 465, 42-51.
- Darquenne, C., 2012. Aerosol deposition in health and disease. *J. Aerosol Med. Pulm. Drug Deliv.* 25, 140-147.
- de Souza Carvalho, C., Daum, N., Lehr, C.-M., 2014. Carrier interactions with the biological barriers of the lung: Advanced in vitro models and challenges for pulmonary drug delivery. *Adv. Drug Delivery Rev.* 75, 129-140.
- Dullien, F.A.L., 1992. *Pore structure, Porous media* 2ed. Academic Press, San Diego, pp. 5-115.
- Dunbar, C., Watkins, A., Miller, J., 1997. An experimental investigation of the spray issued from a pmdi using laser diagnostic techniques. *J. Aerosol Med.* 10, 351-368.
- Edwards, D.A., Hanes, J., Caponetti, G., Hrkach, J., Ben-Jebria, A., Eskew, M.L., Mintzes, J., Deaver, D., Lotan, N., Langer, R., 1997. Large porous particles for pulmonary drug delivery. *Science* 276, 1868 -1871.
- Finlay, W., 2011. Pharmaceutical aerosol sprays for drug delivery to the lungs, in: Ashgriz, N. (Ed.), *Handbook of atomization and sprays: Theory and applications*. Springer, pp. 899-907.



Finlay, W.H., 2001. Metered dose propellant inhalers, The mechanics of inhaled pharmaceutical aerosols. Academic Press, San Diego, pp. 277-293.

Gartlehner, G., Hansen, R.A., Carson, S.S., Lohr, K.N., 2006. Efficacy and safety of inhaled corticosteroids in patients with COPD: A systematic review and meta-analysis of health outcomes. *Ann. Fam. Med.* 4, 253-262.

Grainger, C., Saunders, M., Buttini, F., Telford, R., Merolla, L., Martin, G., Jones, S., Forbes, B., 2012. Critical characteristics for corticosteroid solution metered dose inhaler bioequivalence. *Mol. Pharm.* 9, 563-569.

Gupta, A., Stein, S.W., Myrdal, P.B., 2003. Balancing ethanol cosolvent concentration with product performance in 134a-based pressurized metered dose inhalers. *J. Aerosol Med.* 16, 167-174.

Haghi, M., Bebawy, M., Colombo, P., Forbes, B., Lewis, D.A., Salama, R., Traini, D., Young, P.M., 2014. Towards the bioequivalence of pressurised metered dose inhalers 2. Aerodynamically equivalent particles (with and without glycerol) exhibit different biopharmaceutical profiles *in vitro*. *Eur. J. Pharm. Biopharm.* 86, 38-45.

Hancock, B.C., Shamblin, S.L., Zografi, G., 1995. Molecular mobility of amorphous pharmaceutical solids below their glass transition temperatures. *Pharm. Res.* 12, 799-806.

Hédoux, A., Guinet, Y., Descamps, M., 2011. The contribution of raman spectroscopy to the analysis of phase transformations in pharmaceutical compounds. *Int. J. Pharm.* 417, 17-31.

Hinds, W.C., 1999. *Aerosol technology: Properties, behavior, and measurement of airborne particles*, 2nd ed. Wiley, Hoboken, NJ.

Hobbs, P.V., 1974. *Ice physics*. Oxford New York.

Hoose, C., Möhler, O., 2012. Heterogeneous ice nucleation on atmospheric aerosols: A review of results from laboratory experiments. *Atmos. Chem. Phys.* 12, 9817-9854.

Israelachvili, J.N., 2011. *Adhesion and wetting phenomena, Intermolecular and surface forces*, 3 ed. Academic Press, Burlington, MA.

Ivey, J.W., Lewis, D., Church, T., Finlay, W.H., Vehring, R., 2014. A correlation equation for the mass median aerodynamic diameter of the aerosol emitted by solution metered dose inhalers. *Int. J. Pharm.* 465, 18-24.

Ivey, J.W., Vehring, R., Finlay, W.H., 2015. Understanding pressurized metered dose inhaler performance. *Expert Opin. Drug Deliv.* 12, 901-916.

Kim, C.S., Trujillo, D., Sackner, M., 1985. Size aspects of metered-dose inhaler aerosols 1-3. *Am. Rev. Respir. Dis.* 132, 137-142.

Lange, C.F., Finlay, W.H., 2000. Overcoming the adverse effect of humidity in aerosol delivery via pressurized metered-dose inhalers during mechanical ventilation. *Am. J. Respir. Crit. Care Med.* 161, 1614-1618.

Lechuga-Ballesteros, D., Noga, B., Vehring, R., Cummings, R.H., Dwivedi, S.K., 2011. Novel cosuspension metered-dose inhalers for the combination therapy of chronic obstructive pulmonary disease and asthma. *Future Med. Chem.* 3, 1703-1718.

Lewis, D., Young, P., Buttini, F., Church, T., Colombo, P., Forbes, B., Haghi, M., Johnson, R., O'Shea, H., Salama, R., 2014. Towards the bioequivalence of pressurised metered dose inhalers 1: Design and characterisation of

- aerodynamically equivalent beclomethasone dipropionate inhalers with and without glycerol as a non-volatile excipient. *Eur. J. Pharm. Biopharm.* 86, 31-37.
- Martin, A.R., Finlay, W.H., 2005. The effect of humidity on the size of particles delivered from metered-dose inhalers. *Aerosol Sci. Tech.* 39, 283-289.
- Martin, A.R., Kwok, D.Y., Finlay, W.H., 2005. Investigating the evaporation of metered-dose inhaler formulations in humid air: Single droplet experiments. *J. Aerosol Med.* 18, 218-224.
- Mitchell, J., Nagel, M., Wiersema, K., Doyle, C., Migunov, V., 2003. The effect of humidification on the size distribution of aerosols delivered to the mechanically ventilated patient, 14th International Society for Aerosols in Medicine Congress. Baltimore, MD. *J. Aerosol Med.*, 2004, 16(2): 187-227
- Myrdal, P.B., Sheth, P., Stein, S.W., 2014. Advances in metered dose inhaler technology: Formulation development. *AAPS PharmSciTech* 15, 434-455.
- Oliveira, R.F., Ferreira, A.C., Teixeira, S.F., Teixeira, J.C., Marques, H.C., 2013. Pmdi spray plume analysis: A CFD study, Proceedings of the World Congress on Engineering. International Association of Engineers, London.
- Ooi, J., Gaisford, S., Boyd, B.J., Young, P.M., Traini, D., 2014. Isothermal calorimetry: A predictive tool to model drug-propellant interactions in pressurized metered dose systems. *Int. J. Pharm.* 461, 301-309.
- Roche, N., Dekhuijzen, P.R., 2016. The evolution of pressurized metered-dose inhalers from early to modern devices. *J. Aerosol Med. Pulm. Drug Deliv.* 29, 311-327.
- Ruge, C.A., Kirch, J., Lehr, C.-M., 2013. Pulmonary drug delivery: From generating aerosols to overcoming biological barriers—therapeutic possibilities and technological challenges. *Lancet Respir. Med.* 1, 402-413.
- Sakagami, M., Kinoshita, W., Sakon, K., Sato, J.-I., Makino, Y., 2002. Mucoadhesive beclomethasone microspheres for powder inhalation: Their pharmacokinetics and pharmacodynamics evaluation. *J. Controlled Release* 80, 207-218.
- Sakagami, M., Sakon, K., Kinoshita, W., Makino, Y., 2001. Enhanced pulmonary absorption following aerosol administration of mucoadhesive powder microspheres. *J. Controlled Release* 77, 117-129.
- Schürch, S., Gehr, P., Im Hof, V., Geiser, M., Green, F., 1990. Surfactant displaces particles toward the epithelium in airways and alveoli. *Respir. Physiol.* 80, 17-32.
- Spahn, J.D., 2016. Glucocorticoids, in: Mahmoudi, M. (Ed.), *Allergy and asthma: Practical diagnosis and management*. Springer International Publishing, Basel, pp. 599-622.
- Stein, S., Sheth, P., Hodson, P.D., Myrdal, P., 2014. Advances in metered dose inhaler technology: Hardware development. *AAPS PharmSciTech* 15, 326-338.
- Stein, S.W., 2008. Estimating the number of droplets and drug particles emitted from MDIs. *AAPS PharmSciTech* 9, 112-115.
- Stein, S.W., Myrdal, P.B., 2006. The relative influence of atomization and evaporation on metered dose inhaler drug delivery efficiency. *Aerosol Sci. Tech.* 40, 335-347.
- Tarara, T., Weers, J., Dellamary, L., 2000. Engineered powders for inhalation, *Respiratory Drug Delivery VII*. Serentec Press, Tarpon Springs, FL, p. 413.

Tarara, T.E., Hartman, M.S., Gill, H., Kennedy, A.A., Weers, J.G., 2004. Characterization of suspension-based metered dose inhaler formulations composed of spray-dried budesonide microcrystals dispersed in hfa-134a. *Pharm. Res.* 21, 1607-1614.

Tsapis, N., Bennett, D., Jackson, B., Weitz, D.A., Edwards, D.A., 2002. Trojan particles: Large porous carriers of nanoparticles for drug delivery. *Proc. Natl. Acad. Sci. U.S.A.* 99, 12001 - 12005.

Van Wylen, G., Sonntag, R., 1965. *Fundamentals of classical thermodynamics*, 1 ed. Wiley, New York.

Wang, H., 2015. Low-frequency and macro-raman analysis of respirable dosage forms and their sampling with a low flow rate single-nozzle cascade impactor. M.Sc. thesis, University of Alberta, Edmonton.

Wang, H., Boraey, M.A., Williams, L., Lechuga-Ballesteros, D., Vehring, R., 2014. Low-frequency shift dispersive raman spectroscopy for the analysis of respirable dosage forms. *Int. J. Pharm.* 469, 197-205.

Xu, Z., Hickey, A.J., 2014. The physics of aerosol droplet and particle generation from inhalers, in: Smyth, H.D.C., Hickey, A.J. (Eds.), *Controlled pulmonary drug delivery*. Springer, New York, pp. 75-100.

Zhu, B., Traini, D., Chan, H.-K., Young, P.M., 2013. The effect of ethanol on the formation and physico-chemical properties of particles generated from budesonide solution-based pressurized metered-dose inhalers. *Drug Dev. Ind. Pharm.* 39, 1625-1637.

Zhu, B., Traini, D., Lewis, D.A., Young, P., 2014. The solid-state and morphological characteristics of particles generated from solution-based metered dose inhalers: Influence of ethanol concentration and intrinsic drug properties. *Colloids Surf. A Physiochem. Eng. Asp.* 443, 345-355.